

# TacoGFn: Target-conditioned GFlowNet for Structure-based Drug Design

Tony Shen<sup>1</sup> Seonghwan Seo<sup>2</sup> Grayson Lee<sup>1</sup> Mohit Pandey<sup>3</sup> Jason Smith<sup>3</sup> Artem Cherkasov<sup>3</sup>  
Woo Youn Kim<sup>2,4,5</sup> Martin Ester<sup>1</sup>

## Abstract

Searching the vast chemical space for drug-like and synthesizable molecules with high binding affinity to a protein pocket is a challenging task in drug discovery. Recently, molecular deep generative models have been introduced which promise to be more efficient than exhaustive virtual screening, by directly generating molecules based on the protein structure. However, since they learn the distribution of a limited protein-ligand complex dataset, the existing methods struggle with generating novel molecules with significant property improvements. In this paper, we frame the generation task as a Reinforcement Learning task, where the goal is to search the wider chemical space for molecules with desirable properties as opposed to fitting a training data distribution. More specifically, we propose TACOGFN, a Generative Flow Network conditioned on protein pocket structure, using binding affinity, drug-likeness and synthesizability measures as our reward. Empirically, our method outperforms state-of-art methods on the CrossDocked2020 benchmark for every molecular property (Vina score, QED, SA), while improving the generation time by multiple orders of magnitude. TACOGFN achieves  $-8.82$  in median docking score and 52.63% in Novel Hit Rate.

## 1. Introduction

Structure-based drug design (SBDD) leverages target protein structures to search for high affinity drug molecules.

<sup>1</sup>School of Computing Science, Simon Fraser University, Burnaby, Canada <sup>2</sup>Department of Chemistry, KAIST, Daejeon, Republic of Korea <sup>3</sup>Vancouver Prostate Centre, University of British Columbia, Vancouver, Canada <sup>4</sup>AI Institute, KAIST, Daejeon, Republic of Korea <sup>5</sup>HITS Inc., Seoul, Republic of Korea. Correspondence to: Tony Shen <tsa87@sfsu.ca>.

*Proceedings of the 41<sup>st</sup> International Conference on Machine Learning*, Vienna, Austria. PMLR 235, 2024. Copyright 2024 by the author(s).

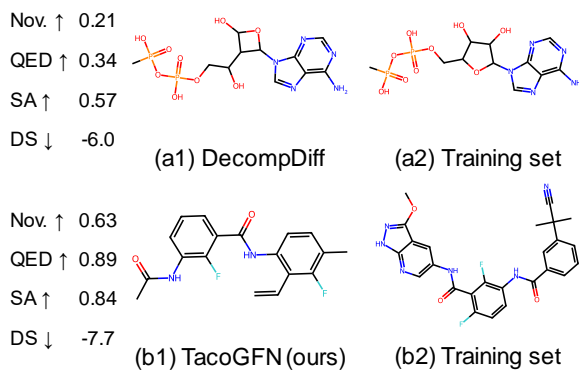


Figure 1. Example of molecules generated for target 5w2g by DecomDiff (Guan et al., 2023b) - a current SOTA baseline (a1) and our model (b1), presented alongside the with the most similar molecule from the training set (a2, b2). Relevant properties of generated molecules are listed:  $\uparrow$  denotes higher is better,  $\downarrow$  denotes lower is better.

Due to the growing availability of protein structures from ML protein structure prediction methods (Jumper et al., 2021), and many novel targets identified from high-throughput perturbation experiments (Replogle et al., 2022), SBDD is becoming an increasingly powerful approach in drug discovery. It currently takes 13-15 years and between US \$2 billion and \$3 billion for a single drug to be developed and approved (Pushpakom et al., 2018). The substantial expense and time of drug development not only impose a significant burden on healthcare systems but also amplify societal risks during global health crises, such as the COVID-19. There is an urgent need to expedite the design of novel drug candidates for new protein targets.

Traditionally, molecular docking has been used to virtually screen libraries of molecules for interaction with a target protein. Its efficacy is impeded by the exhaustive nature of its search, and by the high computational cost of molecular docking. To overcome this challenge, recently deep generative models (Luo et al., 2021; Peng et al., 2022; Guan et al., 2023b) have been proposed to design molecules (ligands) conditioned on a pocket structure. These methods learn the distribution of a training dataset of protein-ligand complex structures.

However, due to the high cost of the experiments, the size

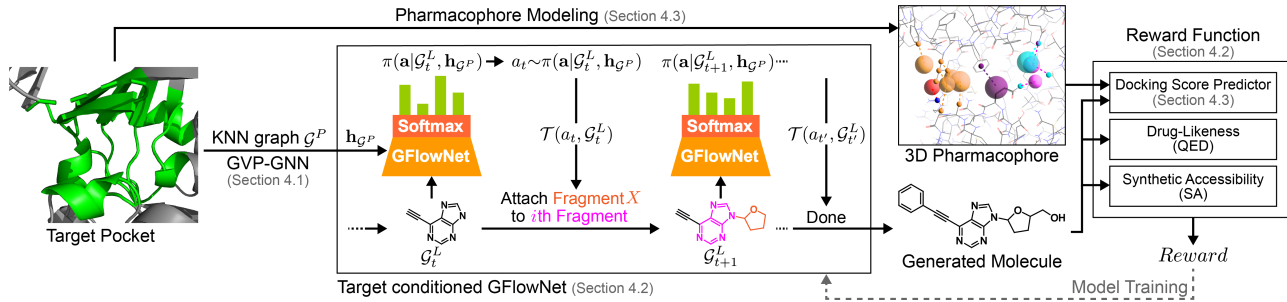


Figure 2. Overview of the sampling and training process of TACOGFN.

of the training datasets for SBDD, i.e. high-quality protein-ligand binding structure data, is relatively small. PDBBind (Liu et al., 2014), the dataset on which the standard CrossDocked2020 benchmark (Francoeur et al., 2020) is based on, contains only 19,443 protein-ligand complexes. After removing common biomolecules and duplicates, only 4,200 unique drug-like molecules remain (Powers et al., 2023). This is only a tiny fraction of the entire chemical space of drug-like molecules that is assumed to consist of  $\sim 10^{60}$  molecules (Lipinski et al., 1997). As a consequence, existing methods of SBDD based on distribution learning have struggled to generate novel molecules with significantly improved properties (Lee et al., 2023), since they generate molecules with high structural similarity to the training set (Guan et al., 2023b).

In this paper, we frame the task of SBDD as a Reinforcement Learning (RL) task, where the goal is to search the chemical space for molecules with desirable molecular properties as opposed to fitting a training data distribution. We propose TACOGFN, a Target Conditioned Generative Flow Network that generates molecules conditioned on a given protein pocket structure, guided by rewards based on predicted affinity of the molecule to the pocket, drug-like properties and synthesizability of the molecule. We introduce a docking score predictor which leverages pre-trained pharmacophore representation to efficiently evaluate millions of diverse protein-ligand pairs during training. We performed an experimental evaluation on the standard CrossDocked benchmark dataset and demonstrated that TACOGFN clearly outperforms state-of-the-art methods. Our method achieved up to  $-8.82$  in median docking score while obtaining far superior values of drug-likeness and synthesizability. Furthermore, TACOGFN reaches a Novel Hit Rate of 52.63%, which is a dramatic improvement over the 7.94% obtained by the best performing baseline model.

To summarize, the main contributions of this paper are:

- We point out the limitations of previous distribution learning approaches and propose to frame pocket-conditioned molecule generation as a multi-objective RL task.
- We propose TACOGFN, which conditions a GFlowNet

for learning a family of molecule distributions conditioned on protein pocket structures.

- We develop a docking score predictor with improved generalization capabilities using a pre-trained pharmacophore representation, enabling fast affinity evaluation.
- TACOGFN clearly outperforms the current SOTA on the CrossDocked2020 benchmark and demonstrates the benefit of our approach over existing distribution learning based methods.

## 2. Related Work

**Structure-based drug design** aims to sample drug-like molecules that fit a given target protein pocket. LiGAN (Masuda et al., 2020) uses 3D CNNs to encode the protein pocket structure and predict atom densities from the encoded latent space. 3DSBDD (Luo et al., 2021) and Pocket2Mol (Peng et al., 2022) adopt an auto-regressive approach to generate molecules atom by atom. Other methods such as FLAG (Zhang et al., 2023b) and DrugGPS (Zhang & Liu, 2023) build molecules fragment by fragment to leverage the chemical prior. A very recent line of research employs diffusion models (Guan et al., 2023a;b; Schneuing et al., 2023) for SBDD. TargetDiff (Guan et al., 2023a) is a diffusion-based method which generates atom coordinates and atom types in a non-autoregressive way, and bonds are generated in a post-processing step. DecompDiff (Guan et al., 2023b) is a diffusion model which generates both atoms and bonds with decomposed priors, which reflect the natural decomposition of a ligand molecule into arms and scaffold. DecompDiff has achieved state-of-the-art performance on the CrossDocked2020 benchmark. A recent analysis paper (Harris et al., 2023) questions the assumption that explicit 3D modelling of the ligand improves performance, after finding a much higher occurrence of physical violations and fewer key interactions in molecules generated using 3D modelling. In our work, we generate molecules in 2D space to vastly reduce the search space and compute time; Our approach is shown to effectively leverage the target pocket structure for generating molecules with high affinity.

**Goal-directed molecule generation** aims to generate molecules that satisfy certain optimization goals such as strong binding affinity and high drug-likeness. Reinforcement Learning (RL) methods such as ReLeaSE (Olivcrona et al., 2017), MolDQN (Zhou et al., 2019) and REINVENT (Blaschke et al., 2020) have been proposed to guide the generation of molecules toward desirable properties. MORLD (Jeon & Kim, 2020) and MoleGuLAR (Goel et al., 2021) combine RL and docking calculations to design novel ligands. MOOD (Lee et al., 2023) incorporates out-of-distribution and property-guided exploration in diffusion models for goal-directed molecule generation. Existing goal-directed methods are constrained by a fixed objective function. They are trained to generate high-affinity molecules for a single target pocket, and therefore, a new model is needed for each different protein pocket. In contrast, TACOGFN is conditioned on a protein pocket graph and is trained to generate high-affinity molecules for any pocket structure.

**Protein-ligand affinity prediction.** Predicting the affinity or the docking score of a ligand to a target, in the absence of their binding complex structure, is a difficult task. Most previous docking score prediction models have been limited to a single protein target (Bengio et al., 2021; Gentile et al., 2020). Therefore, they are not suitable for the aim of designing high-affinity molecules for any given protein pocket structure. Recently, several methods have been proposed to predict ligand affinity for arbitrary protein targets (Zhang et al., 2023a; Pandey et al., 2022). However, these approaches are prone to memorizing the structural bias instead of learning the physics of protein-ligand binding and show low generalization ability to unseen ligands or proteins (Wallach & Heifets, 2018; Chan et al., 2023). To this end, we adopt a pre-trained pharmacophore representation, which only models the key interaction sites for a protein pocket. This prior improves our docking score predictor’s ability to learn physical interactions and generalize to unseen data.

### 3. GFlowNet Preliminaries

Generative Flow Networks (GFlowNets, GFN) (Bengio et al., 2021) learn a stochastic policy  $\pi$  for generating a combinatorial object (such as molecular graph)  $x \in \mathcal{X}$ . The probability of constructing  $x$ , denoted as  $\pi(x)$ , is trained to be proportional to a non-negative reward function  $R : \mathcal{X} \mapsto \mathbb{R}^+$  defined on the space  $\mathcal{X}$ . This property of GFlowNet is ideal for generating diverse molecules with desirable properties. Conditional GFlowNet introduced in (Jain et al., 2023) simultaneously model a family of reward functions. Each conditional information, denoted as  $c \in \mathcal{C}$ , induces a unique reward function  $R(x|c)$ . In our work, we adopt conditional GFlowNet for SBDD settings, by encoding target pocket structure as condition  $c$ . Thus, a single

GFlowNet models high-reward molecule distribution across all protein pockets.

Each object  $x$  is constructed from a sequence of actions  $a \in \mathcal{A}$ . In molecular settings, a molecule is constructed by inserting molecule fragments into a partially constructed fragment graph state  $s \in \mathcal{S}$  (Bengio et al., 2021). Conceptually, a GFlowNet is an acyclic graph  $G = (\mathcal{S}, \mathcal{E})$ , with nodes  $\mathcal{S}$  and edges  $\mathcal{E}$ . Each transition  $s \rightarrow s' \in \mathcal{E}$  via action  $a \in \mathcal{A}$  corresponds to an edge in graph  $G$ . The transition function  $\mathcal{T} : \mathcal{S}, \mathcal{A} \mapsto \mathcal{S}$  computes the new state  $s' = \mathcal{T}(s, a)$  given action  $a$  on state  $s$ . A special action moves state  $s$  into terminating states  $\mathcal{X} \subset \mathcal{S}$ . We define the initial empty graph as  $s_0$ . Construction of  $x$  can be defined over a trajectory of states  $\tau = (s_0 \rightarrow s_1 \rightarrow \dots \rightarrow x)$ .

The forward policy  $P_F(s'|s, c)$  of a GFlowNet represents the probability distribution of reaching state  $s'$  from state  $s$  conditioned on context  $c$ . Partition function  $Z(c)$  is the sum of the rewards  $R(x|c)$  for all objects  $x \in \mathcal{X}$ . We adopt the Trajectory Balance objective from Equation 1 to efficiently learn a forward policy  $P_F$  that generates object  $x$  with probability proportional to its reward  $R(x|c)$  (Malkin et al., 2023).

$$\mathcal{L}_{TB}(\tau, c; \theta) = \left( \log \frac{Z_\theta(c) \prod_{s \rightarrow s' \in \tau} P_{F_\theta}(s'|s, c)}{R(x|c)} \right)^2, \quad (1)$$

$\theta$  represents the learnable parameters. Our goal is to learn a policy  $\pi(x|c) \approx \frac{R(x|c)}{Z(c)}$  across all molecules  $x \in \mathcal{X}$  and protein pocket contexts  $c \in \mathcal{C}$ .

### 4. TacoGFN

**Problem definition.** The goal of structure-based drug design is to generate molecules with both desirable properties and strong binding affinity with respect to a given protein pocket structure. The pocket structure is denoted as  $p$  and will be represented as a  $K$ -nearest neighbor (KNN) residue graph. The ligand is denoted as  $l$  and will be represented either as an atom graph or a fragment graph. We define a reward function  $R(l|p)$  based on a molecule’s predicted docking score, drug-likeness and synthesizability. Our goal is to learn a molecule generation policy that constructs molecules  $l$  given protein structure  $p$  with probability matching their reward, such that  $\pi(l|p) \propto R(l|p)$ .

Since TACOGFN’s training objective is based on the reward and not a fixed dataset, it explores a much greater chemical space and discovers novel molecules beyond the known data distribution. In addition, by matching the generation probability to the reward, TACOGFN can discover molecules that improve multiple objectives compared to the training data distribution. In summary, TACOGFN explores the wider chemical space for high reward candidates instead of memorizing a small set of known binding molecules.

**Method overview.** TACOGFN is a single conditioned generative model that generalizes over protein pockets. It explores the greater chemical space to generate high-affinity molecules with properties desirable as a drug candidate. The protein pocket is first featurized as a  $K$ -nearest neighbor residue graph and encoded using GVP-GNN (Jing et al., 2021) (section: 4.1). Then, we use this pocket embedding as the condition for GFlowNet molecule generation (section 4.2). Finally, we reward generated molecules using our docking score prediction model which leverages protein-ligand interaction priors (section 4.3). The high-level architecture of our SBDD framework is illustrated in Figure 2.

#### 4.1. Pocket structure encoder

We represent structure of the pocket  $p$  as a standard  $K$ -nearest neighbor (KNN) residue graph  $\mathcal{G}^P = (\mathcal{V}^P, \mathcal{E}^P)$  - following previous work in protein representation (Jing et al., 2021). The  $i$ -th residue node  $v_i^P \in \mathcal{V}^P$  is featurized using its geometric and chemical properties. These features include the type of residue, the dihedral angles of the atoms in the residue backbone, and the directional unit vectors. An edge  $e_{ij}^P \in \mathcal{E}^P$  is formed if the  $j$ -th residue  $v_j^P$  is among the  $K$ -nearest neighbors of residue  $v_i^P$ , as measured by the euclidean distance between their respective  $C_a$  atoms. We set the number of neighbours  $K = 30$ . An edge is featurized with the Euclidean distance, distance along the backbone and the direction vector between the two residues. These features sufficiently describe the features of the protein pocket.

We apply a graph neural network with geometric vector perceptrons (GVP) layers (Jing et al., 2021) to the KNN pocket graph  $\mathcal{G}^P$  to learn the node embedding  $\mathbf{h}_{v_i^P}$  for each residue. The node embeddings  $\{\mathbf{h}_{v_i^P}\}$  are then averaged to obtain an embedding of the entire graph  $\mathbf{h}_{\mathcal{G}^P}$ . We use GVP because it encodes the protein pocket into an embedding that is invariant to rotations and translations.

#### 4.2. Pocket conditioned GFlowNet

In this section, we discuss how to employ the pocket structure, more specifically its latent embedding, to condition the GFlowNet to generate molecules that interact with a given protein pocket. Furthermore, we describe our fragment-based molecular generation framework.

**Molecule representation.** During molecular generation, we represent ligands as a 2D molecular graph  $\mathcal{G}^L = (\mathcal{V}^L, \mathcal{E}^L)$  with node  $v_i^L \in \mathcal{V}^L$  representing a molecule fragment, and directional edges  $e_{ij}^L \in \mathcal{E}^L$  indicating the attachment atom of fragment  $v_i^L$  that connects to fragment  $v_j^L$ . Since a molecule’s desirability as a drug in the real world is independent of its *predicted* 3D conformation, the 2D representation of a ligand here is appropriate.

**Fragment vocabulary construction.** TACOGFN generates molecules by adding one molecular fragment at a time. To create the vocabulary of fragments used, we extract common fragments from a chemical database in a data-driven and chemically valid way. To obtain a fragment vocabulary, we first apply BRICS decomposition (Degen et al., 2008) to 250k ZINC20 (Irwin et al., 2020) molecules. BRICS breaks molecules via retrosynthetic rules and provides synthetically accessible building blocks, i.e. molecules that are easy to prepare (Seo et al., 2023). To reduce the fragment vocabulary size, we further break all single bonds connecting a heavy atom to a ring structure. Next, we retain the fragments that occur in more than 50 (0.02%) of the molecules in our ZINC sample. Finally, we merge identical fragment graphs. Attachment points are atoms with a broken bond resulting from the molecule decomposition. This results in a set of 475 building block-like fragments. As our fragments are mined from a synthetically accessible virtual library, TACOGFN can generate more synthesizable and chemically valid molecules compared to atom-based construction methods.

**Molecular generation framework.** We formulate molecular generation as a sequential decision process and implement it using a GFlowNet. At the  $t$ -th step, the policy  $\pi$  samples an action  $a$  depending on the current molecule state  $\mathcal{G}_t^L$  and pocket embedding  $\mathbf{h}_{\mathcal{G}^P}$ . The transition function  $\mathcal{T}$  is a deterministic function which applies the action to the molecular graph at step  $t$  to produce a molecule graph at step  $t + 1$ .

$$a_t \sim \pi(a | \mathcal{G}_t^L, \mathbf{h}_{\mathcal{G}^P}) \quad (2)$$

$$\mathcal{G}_{t+1}^L = \mathcal{T}(a_t, \mathcal{G}_t^L) \quad (3)$$

Previous autoregressive models often formulate action prediction as a supervised task, where the goal is to predict the correct ground truth actions obtained from masked molecules (Peng et al., 2022). Instead, our molecule generation policy  $\pi$  aims to generate molecules with probability  $P(\mathcal{G}^L | \mathbf{h}_{\mathcal{G}^P})$  proportional to the reward.

**Pocket conditioned molecular generation.** Here, we adopt the architecture for molecular generation introduced in Multi-Objective GFlowNet (MO-GFN) (Jain et al., 2023). Instead of conditioning the GFlowNet on multi-objective preference, we condition the GFlowNet on pocket embeddings to learn a family of molecular distributions corresponding to a family of reward functions induced from the pocket structure diversity.

We use a graph transformer (Yun et al., 2020) to model our policy  $\pi(a | \mathcal{G}_t^L, \mathbf{h}_{\mathcal{G}^P})$ , by taking the partially constructed molecular graph at the  $t$ -th time step  $\mathcal{G}_t^L$  and the pocket embedding  $\mathbf{h}_{\mathcal{G}^P}$  as input. The input feature  $\mathbf{h}_i^{L(0)}$  of molecular node  $v_i^L$  is a one-hot encoding of the node’s fragment type. The molecular edge input feature  $\mathbf{e}_{ij}^{L(0)}$  is a one-hot

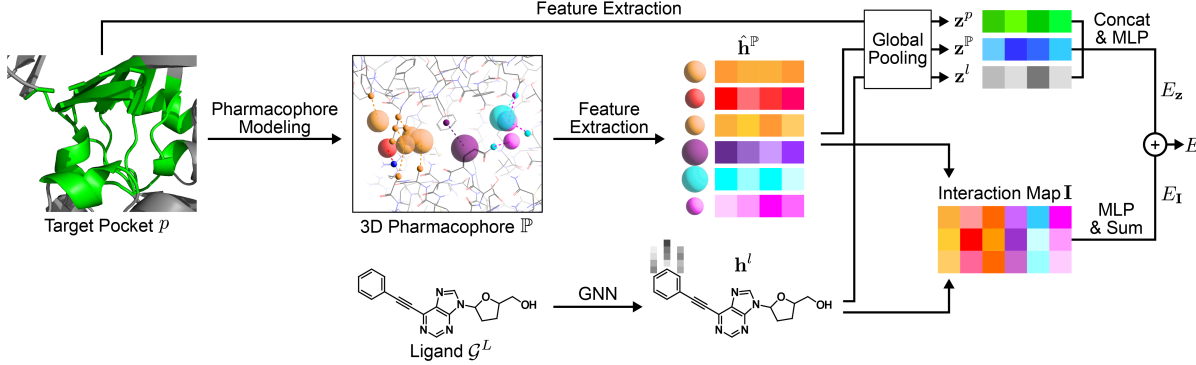


Figure 3. Model architecture of the docking score predictor. Each pharmacophore point is represented as a sphere and corresponds to a desired ligand characteristic for a binding interaction.

mapping of the attachment atom index in node  $v_i^L$  which connects to node  $v_j^L$ . We add an additional virtual conditioning node  $\mathbf{h}^{V(0)}$ , featurized using pocket embedding  $\mathbf{h}_{GP}$ , to the graph  $\mathcal{G}_t^L$  (Pham et al., 2017). This virtual node is connected to all other nodes and serves as a graph-level node to provide pocket information. After  $N$  Transformer layers, the set of final node embeddings  $\{\mathbf{h}_i^{L(N)}$  and edge embeddings  $\{\mathbf{e}_{ij}^{L(N)}$  are obtained. The final graph level embedding  $\mathbf{g}^{L(N)}$  is obtained via the concatenation of the global average pooling of the node embeddings and the final virtual node embedding  $\mathbf{h}^{V(N)}$ , as seen in Equation 4.

$$\mathbf{g}^{L(N)} = \text{Concat} \left( \text{AvgPool} \left( \{\mathbf{h}_i^{L(N)}\} \right), \mathbf{h}^{V(N)} \right) \quad (4)$$

Using these final molecular graph embeddings, we sample from the following three action types defined in previous works on fragment-based molecular generation (Bengio et al., 2021; Jin et al., 2018): 1) *Fragment addition* is a node action that connects the current node to a new node via a new edge. An MLP is applied on the node embeddings  $\mathbf{h}_i^{L(N)}$  to produce logits over the fragment vocabulary for every node in the molecular graph. 2) *Attachment specification* is an edge action that specifies the attachment atom in a node (fragment) which will form a single bond with the other fragment. An MLP is applied on each edge embedding  $\mathbf{e}_{ij}^{L(N)}$  to produce logits over attachment point choices. 3) *Stop construction* is a graph action that marks the finish of a molecule. The logit is produced from a single MLP output based on the final graph embedding  $\mathbf{g}^{L(N)}$ . All logits are concatenated and scaled into probabilities using the softmax function, and an action is sampled from the distribution (see Equations in B.1). The same process is repeated for each time step until the *stop construction* action is sampled.

**Reward function.** A drug candidate must not only have a high affinity to the pocket but also satisfy drug-like properties and synthetizability requirements to be selected for experimental validation. We design a reward function which combines all three aspects, using QED (Bickerton et al.,

2012) as a measure of drug-likeness, SA (Ertl & Schuffenhauer, 2009) as a measure of ease-of-synthesizability, and predicted docking score as a measure of affinity between ligand and protein (see details in Appendix B.2). Computing the reward is very fast, for example, computing it for a batch of 64 protein-ligand pairs took under 0.15 seconds.

#### 4.3. Docking score predictor with pharmacophore prior

The exploration of chemical space with a GFlowNet requires evaluating binding affinities for millions of molecules sampled during training. However, using molecular docking for evaluation is computationally expensive. Here, we propose a fast ML-based docking score predictor that generalizes well across molecule and protein pocket distributions, as described in Figure 3 and Equation 5. (See details in Appendix C)

We leverage PharmacophoreNet (Seo & Kim, 2023), a recent deep learning method to obtain the pharmacophore  $\mathbb{P}$  from a pocket structure  $p$ .<sup>1</sup> To enrich the representation, we obtained the embedding of the pocket  $\mathbf{z}^p$  and the embeddings of pharmacophore points  $\{\hat{\mathbf{h}}_i^{\mathbb{P}}\}$  from PharmacophoreNet. The 1D representation vectors of the pharmacophore  $\mathbf{z}^{\mathbb{P}}$  is computed by the global pooling of  $\{\hat{\mathbf{h}}_i^{\mathbb{P}}\}$ .

During docking score prediction, we represent a ligand as an atom-level 2D molecular graph. We apply Graph Isomorphism Network (Hu et al., 2019) to the atom graph to obtain the node embeddings  $\{\mathbf{h}_i^L\}$ .  $\mathbf{z}^L$  is a 1D representation vector of the ligand, obtained by the global pooling of node embeddings  $\{\mathbf{h}_i^L\}$ . Then, we incorporate a pairwise interaction map  $\mathbf{I}$  - computed from the outer product of  $\{\hat{\mathbf{h}}_i^{\mathbb{P}}\}$  and  $\{\mathbf{h}_i^L\}$ . This preserves the structural topology and binding interaction details. Notably, our docking score predictor

<sup>1</sup>Pharmacophore is a point set, where each point describes the desirable motif properties (such as being aromatic) a ligand should possess at this geometric position to form energetically or entropically favourable interactions (e.g.  $\pi-\pi$  stacking) with the protein target. (Wermuth et al., 1998; Yang, 2010).

uses the pharmacophore points involved in binding instead of atoms or amino acids to obtain the interaction map. It improves the generalization ability at a reduced computational cost through coarse-grained modelling of the pocket at the pharmacophore level.

$$E = \phi_z(\text{Concat}(\mathbf{z}^p, \mathbf{z}^{\mathbb{P}}, \mathbf{z}^l)) + \text{SumPool}(\phi_{\mathbf{I}}(\mathbf{I})) \quad (5)$$

## 5. Experiments

### 5.1. Datasets

We train the docking score predictor on datasets containing protein-ligand pairs and their corresponding Quick Vina 2.1 (QVINA) docking scores. We consider two datasets to train our predictor. The first dataset - **CrossDock-100k** is commonly used in previous works (Luo et al., 2021; Peng et al., 2022; Guan et al., 2023b). We first apply identical splitting and processing protocol on the CrossDocked dataset (Francoeur et al., 2020) to obtain the same split of 100k protein-ligand pairs (See details in Appendix D.1). We then dock and score using Quick Vina 2.1 (QVINA) (Trott & Olson, 2010; Alhossary et al., 2015) for all protein-ligand pairs from this training split. For our purpose of training a docking score predictor, we do not require high-quality protein-ligand structural data such as the CrossDock-100k set. Thus, we introduce a second, novel dataset for docking score prediction more suited for our method called **ZINCDock-15M**. It consists of about 15M docking simulation data - from docking 1,000 random ZINC20 (Irwin et al., 2020) molecules into each of the 15,207 unique pockets from CrossDock-100k training split using QVina.

We could directly compare our molecular generation performance with existing methods when trained on CrossDock-100k, as we train on the same set of protein-ligand complexes. However, we could not fairly train existing methods on the new ZINCDock-15M dataset. Instead of containing experimental-like structure data between known binders and their target, ZINCDock-15M contains random molecules docking conformation in protein pockets. Learning a distribution of random molecules with a distribution learning objective is likely unhelpful for generating high-affinity binding molecules. Our method’s advantage here is that we benefit strongly from this large-scale docking data.

### 5.2. Evaluation settings

For all experiments, each method is tasked to produce 100 unique and valid molecules (ligands) for each of the 100 protein pockets from the CrossDock-100k test set.

**Evaluation metrics.** The goal of structure-based drug discovery is to propose novel drug candidates. Importantly, a drug candidate must simultaneously have high affinity, desirable drug-like properties, and be easily synthesizable to be

considered for further (expensive) experimental validation. To evaluate these molecular properties, the following metrics are commonly used: (1) **Docking Score (DS)** approximates the binding energy between a generated molecule and a protein pocket, where a lower docking score indicates a higher binding affinity. Molecules are docked using QVina (Trott & Olson, 2010; Alhossary et al., 2015) (See Appendix D.2 for details). (2) **QED** is a measure of drug-likeness, estimating a molecule’s suitability as an oral drug based on its properties (Bickerton et al., 2012). (3) **Synthetic Accessibility (SA)** estimates difficulty of synthesizing the molecule (Ertl & Schuffenhauer, 2009). The score is normalized between 0 and 1 using the formula  $(10 - SA)/9$ .

We report the average of these performance metrics in Table 2. However, presenting only the averages of these property values is insufficient, as it ignores whether any individual molecule simultaneously satisfies all of the necessary requirements (Lee et al., 2023). Nor does it evaluate the ability of the model to generate novel structures, which is important for avoiding already patented scaffolds or known binders as noted in (Schreyer & Blundell, 2012).

Therefore, following previous work in *de novo* drug discovery (Lee et al., 2023), we define a *desirable* (*desr.*) molecule candidate for drug as a molecule with a  $\text{QED} > 0.5$ , and an  $\text{SA} > 0.5$ . A *hit* molecule is defined as a molecule with a Docking Score (DS)  $< -8.0$  in addition to satisfying the *desirable* requirements. Lastly, the *novelty* (*nov.*) constraint selects molecules with a maximum Tanimoto similarity  $< 0.5$  with the CrossDocked training molecules, which represent the known binder set. We employ the following additional metrics to better reflect the drug discovery objectives: (4) **Hit (%)** is the fraction of generated molecules that satisfy the *hit* constraint. (5) **Novel Hit (%)**, introduced in (Lee et al., 2023), is the fraction of generated molecules that satisfy both the *novelty* and *hit* constraint. (6) **Top-10 DS** is the average of top 10 docking scores of all generated molecules. (7) **Top-10 Desr. DS** is the average of the top 10 docking scores of generated molecules that satisfy the *desirable* constraint. (8) **Novelty** (Lee et al., 2023; Peng et al., 2022) is the average Tanimoto distance of molecules to the nearest ligand from the CrossDocked training set (known binders) (Bajusz et al., 2015). (9) **Diversity** is calculated as the average pairwise fingerprint Tanimoto distance between molecules generated for a pocket. (9) **Time** is the average runtime (in seconds) for generating 100 unique and valid molecules for a pocket.

**Baselines.** We compare TACOGFN against several state-of-the-art SBDD methods. In particular, we select three recent methods - **Pocket2Mol** (Peng et al., 2022), **TargetDiff** (Guan et al., 2023a), **DecompDiff** (Guan et al., 2023b) and reproduce their experimental results (See Appendix D.4 for details). Except for the results of these three methods, all

Table 1. Evaluation of 100 generated molecules for each of 100 protein pockets from the CrossDocked test set. The best results are in bold and the second best results are underlined. The average and median values are calculated over the averages for each pocket.

Model	Hit % ( $\uparrow$ )	Novel Hit % ( $\uparrow$ )		Top-10 DS ( $\downarrow$ )		Top-10 desir. DS ( $\downarrow$ )		Nov. ( $\uparrow$ )		Div. ( $\uparrow$ )		Time ( $\downarrow$ )
		Avg.	Med.	Avg.	Med.	Avg.	Med.	Avg.	Med.	Avg.	Med.	
Random ZINC	28.88	17.86		-9.12	-9.23	-9.05	-9.16	0.55	0.55	0.76	0.76	-
Pocket2Mol (Peng et al., 2022)	20.85	6.79		-9.10	-8.4	-8.47	-8.23	0.45	0.46	<u>0.74</u>	<b>0.77</b>	2503
TargetDiff (Guan et al., 2023a)	15.65	7.94		-9.40	-9.54	-8.52	-8.70	0.49	0.49	<u>0.74</u>	<u>0.73</u>	3428
DecompDiff (Guan et al., 2023b)	8.95	3.01		-9.79	-9.69	-4.92	-5.28	0.45	0.45	0.60	0.60	6189
TACOGFN (ours)	<u>58.25</u>	<u>43.49</u>		<u>-9.97</u>	<u>-10.26</u>	<u>-9.96</u>	<u>-10.26</u>	<u>0.52</u>	<u>0.52</u>	0.53	0.53	<b>4.29</b>
TACOGFN <sub>Ranked</sub> (ours)	<b>66.02</b>	<u>52.63</u>		<u>-10.30</u>	<u>-10.54</u>	<u>-10.30</u>	<u>-10.54</u>	<u>0.53</u>	<u>0.53</u>	0.49	0.49	21.40

Table 2. Comparison of the properties of the reference molecules and the generated molecules for the CrossDocked test set pockets. The reference molecules are from the CrossDocked test set.

Model	DS ( $\downarrow$ )		QED ( $\uparrow$ )		SA ( $\uparrow$ )	
	Avg.	Med.	Avg.	Med.	Avg.	Med.
Reference	-7.45	-7.26	0.48	0.47	0.73	0.74
LiGAN (Masuda et al., 2020)	-6.33	-6.20	0.39	0.39	0.59	0.57
GraphBP (Liu et al., 2022)	-4.80	-4.70	0.43	0.45	0.49	0.48
3DSBDD (Luo et al., 2021)	-6.75	-6.62	0.51	0.50	0.63	0.63
Pocket2Mol (Peng et al., 2022)	-7.49	-7.00	0.57	0.58	0.75	0.76
TargetDiff (Guan et al., 2023a)	-7.36	-7.56	0.49	0.49	0.60	0.59
DiffSBDD (Schneuing et al., 2023)	-7.33	-	0.47	-	0.55	-
FLAG (Zhang et al., 2023b)	-7.25	-7.17	0.50	0.51	0.75	0.72
DrugGPS (Zhang & Liu, 2023)	-7.36	-7.42	0.59	0.58	0.72	0.73
DecompDiff (Guan et al., 2023b)	<u>-8.35</u>	-8.25	0.37	0.35	0.56	0.56
TACOGFN (ours)	-8.25	<u>-8.39</u>	<b>0.67</b>	<b>0.67</b>	<u>0.79</u>	<u>0.79</u>
TACOGFN <sub>Ranked</sub> (ours)	<b>-8.63</b>	<u>-8.82</u>	<u>0.67</u>	<u>0.67</u>	<b>0.80</b>	<b>0.80</b>

other evaluation results are taken from the recent SBDD survey paper (Zhang et al., 2023c). Furthermore, we randomly select 100 molecules from ZINC20 to form our baseline **Random ZINC**.

TACOGFN is trained using rewards computed by the docking score predictor trained on the CrossDock-100k dataset for a fair comparison. TACOGFN<sub>Ranked</sub> is identical to TACOGFN, except that it generates 500 molecules, and returns only the top 100 molecules with the highest *predicted* docking score according to our docking score predictor. The reported runtimes include both the generation time and the docking score prediction time.

### 5.3. Experimental results

Table 1 and Table 2 present the aggregate of metrics highly important for the objective of *de novo* structure-based drug design. We examine the docking score performances for individual pockets in Figure 4 and show examples of generated molecules in appendix Figure 5. Lastly, we conduct ablation studies to show the benefits of using a larger docking score dataset in Table 3 and validate the utility of the pocket conditioning in Table 4.

**De novo drug design.** Table 1 shows that TACOGFN achieves an impressive hit rate of 58.25%, a large improvement compared to Pocket2Mol (20.85%). Notably, TACOGFN achieves the best average for Top-10 DS ( $-9.97$ ). It also has a significantly improved Top-10 *desirable*

DS ( $-9.96$ ) compared to the second best method TargetDiff ( $-8.52$ ). Since the vast majority of molecules generated by TACOGFN have good QED and SA values, we observe only a tiny decrease in Top-10 DS average when we filter for *desirable* molecules only. In contrast, the Top-10 DS average noticeably drops for all baseline methods if we consider only *desirable* molecules. Finally, we note that TACOGFN is the only method that consistently outperforms the Random ZINC baseline in terms of all affinity-focused metrics, i.e. except novelty and diversity.

Furthermore, TACOGFN achieves an impressive 5-fold improvement in the novel hit rate compared to the state-of-the-art methods. It also achieves the best novelty amongst the three selected representative SBDD methods. These results demonstrate our approach is able to search the greater chemical space and discover highly novel hit molecules, instead of memorizing the training set.

In Table 2, we show that TACOGFN and its variant outperform all baselines in terms of average and median of docking score, QED and SA. This confirms that TACOGFN can generate high-affinity molecules that simultaneously satisfy the drug-likeness and ease-of-synthesis requirements.

As reported in Table 1, the molecules generated by TACOGFN for one particular pocket have lower diversity than those generated by the distribution learning methods that do not attempt to satisfy multiple objectives. As TACOGFN seeks to generate molecules that satisfy multiple property requirements and bind strongly to a specific pocket structure, the resulting solution set is inevitably smaller, resulting in reduced diversity.

Figure 4 shows that TACOGFN achieves better average Top-10 docking scores than DecompDiff in 58% of the test pockets. Notably, the top molecules generated by TACOGFN consistently demonstrate high QED values, whereas the top molecules generated by DecompDiff are characterized by a low QED value. This figure shows that TACOGFN achieves superior docking scores without compromising the drug-like properties across all pocket structures. In appendix Figure 5, we show TACOGFN is able to generate molecules with significantly improved docking scores compared to native ligands.

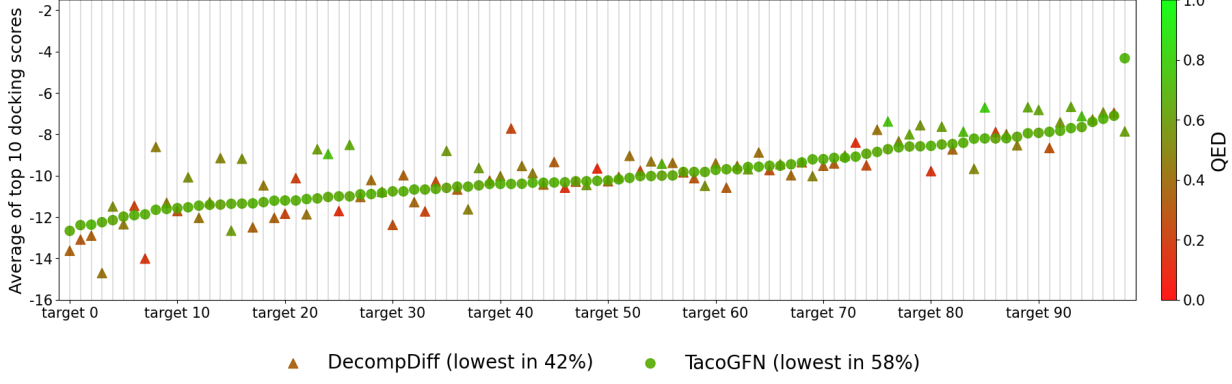


Figure 4. The average of the top-10 docking score of molecules generated for individual CrossDocked test pockets (target) by DecomDiff and TACOGFN. Targets are sorted by the average of the top-10 docking score of TACOGFN generated molecules. A lower docking score means a higher estimated binding affinity. Color is used to denote the average QED value of molecules in the Top-10 set. A higher QED indicates the molecule is more drug-like.

**Generation runtime and quality.** The generation process of TACOGFN is a few orders of magnitude faster than existing autoregressive or diffusion-based generative methods. Additionally, TACOGFN achieves 100% in validity and uniqueness, demonstrating the efficiency of our generation framework. As shown in Table 8 of Appendix D.5.2, this is a significant improvement over previous methods which often generate invalid or duplicate molecules.

**Inference time ranking of generated molecules.** By leveraging the docking score predictor at inference time, TACOGFN<sub>Ranked</sub> further improves our average docking score to  $-8.63$  and the average Top-10 docking score to  $-10.3$ . It also increases the hit rate and novel hit rate up to 66.02% and 52.63% respectively. TACOGFN<sub>Ranked</sub> demonstrates a noticeable improvement in both docking scores and hit rates when we generate a larger set of initial candidates. Compared to the generation time of the fastest baseline model - Pocket2Mol, TACOGFN<sub>Ranked</sub> is still over 100 fold faster. This high speed opens up new applications such as generating a large set of potential binding candidates for down-stream screening using molecular docking or docking score predictors.

#### 5.4. Ablation studies

**Effects of using a larger dataset.** Here, we study the effect of training the docking score predictor on a larger dataset for *de novo* drug design. As shown in Table 3, TACOGFN using the docking score predictor trained on the larger ZINCDock-15M dataset demonstrates significant improvement in average docking score and Novel Hit %. This confirms it is possible to leverage the easily generated large-scale docking score data to generate more novel and higher affinity molecules.

**Effects of pocket conditioning.** To examine the effect of the proposed pocket conditioning for GFlowNet, we train a

Table 3. Evaluation of *de-novo* drug design performance of TACOGFN using docking score predictors trained on two different docking score datasets.

Model	Docking score dataset	DS ( $\downarrow$ )		Top-10 DS ( $\downarrow$ )		Novel Hit % ( $\uparrow$ )
		Avg.	Med.	Avg.	Med.	
TACOGFN	CrossDock-100k	-8.25	-8.39	-9.97	<b>-10.26</b>	58.25
TACOGFN	ZINCDock-15M	<b>-8.35</b>	<b>-8.53</b>	<b>-9.97</b>	-10.22	<b>60.55</b>

molecular generation policy unconditioned on pocket information. The docking score predictor is unchanged - meaning it still predicts a docking score for a molecule with pocket information. The results are shown in Table 4. We observe that the pocket-conditioned GFlowNet achieves higher docking scores compared to the GFlowNet without pocket conditioning. This ablation validates that our method is indeed leveraging pocket conditioning to learn a family of molecular distribution across different pocket structures.

Table 4. Effectiveness of pocket structure conditioning.

Model	Docking score dataset	DS ( $\downarrow$ )		Top-10 DS ( $\downarrow$ )	
		Avg.	Med.	Avg.	Med.
TACOGFN	ZINCDock-15M	<b>-8.35</b>	<b>-8.53</b>	<b>-9.97</b>	<b>-10.22</b>
w/o pocket conditioning	ZINCDock-15M	-8.04	-8.18	-9.65	-9.81

## 6. Conclusion

In this paper, we have investigated the problem of structure-based drug design. To address the limitations of methods based on distribution learning, we have framed pocket-conditioned molecule generation as a multi-objective RL task. We have proposed TACOGFN, a target-conditioned GFlowNet which explores the chemical space to generate novel molecules with high binding affinity and desired properties such as drug-likeness. We have further introduced a docking score predictor using pharmacophore priors, to quickly compute an affinity reward for molecules. Our experiments on the CrossDocked2020 benchmark have demonstrated that TACOGFN outperforms the state-of-the-

art methods in terms of docking scores, percentage of hits, and percentage of novel hits. This demonstrates the potential of TACOGFN as a powerful tool for structure-based drug discovery. In future work, we plan to validate the top generated ligands for some clinically relevant protein pockets *in-vitro*, i.e. in wet-lab experiments.

## Impact statements

This paper presents work whose goal is to advance Machine Learning methods for drug discovery. Such methods are increasingly being employed in the pharmaceutical industry, since they promise to greatly speed-up the lengthy process of drug discovery and to significantly reduce its huge cost. If that promise holds, these Machine Learning methods will benefit patients through better care and our society through a reduction of the economic burden of drug development.

## References

Alhossary, A., Handoko, S. D., Mu, Y., and Kwoh, C.-K. Fast, accurate, and reliable molecular docking with quickvina 2. *Bioinformatics*, 31(13):2214–2216, 2015.

Bajusz, D., Rácz, A., and Héberger, K. Why is tanimoto index an appropriate choice for fingerprint-based similarity calculations? *Journal of cheminformatics*, 7(1):1–13, 2015.

Bender, B. J., Gahbauer, S., Luttens, A., Lyu, J., Webb, C. M., Stein, R. M., Fink, E. A., Balias, T. E., Carlsson, J., Irwin, J. J., and Shoichet, B. K. A practical guide to large-scale docking. *Nature Protocols*, 16(10): 4799–4832, September 2021. ISSN 1750-2799. doi: 10.1038/s41596-021-00597-z. URL <http://dx.doi.org/10.1038/s41596-021-00597-z>.

Bengio, E., Jain, M., Korablyov, M., Precup, D., and Bengio, Y. Flow network based generative models for non-iterative diverse candidate generation, 2021.

Bickerton, G. R., Paolini, G. V., Besnard, J., Muresan, S., and Hopkins, A. L. Quantifying the chemical beauty of drugs. *Nature Chemistry*, 4(2):90–98, January 2012. ISSN 1755-4349. doi: 10.1038/nchem.1243. URL <http://dx.doi.org/10.1038/nchem.1243>.

Blaschke, T., Arús-Pous, J., Chen, H., Margreitter, C., Tyrchan, C., Engkvist, O., Papadopoulos, K., and Patronov, A. REINVENT 2.0: An AI tool for de novo drug design. *Journal of Chemical Information and Modeling*, 60 (12):5918–5922, October 2020. doi: 10.1021/acs.jcim.0c00915. URL <https://doi.org/10.1021/acs.jcim.0c00915>.

Chan, L., Verdonk, M., and Poelking, C. Embracing assay heterogeneity with neural processes for markedly improved bioactivity predictions. *arXiv preprint arXiv:2308.09086*, 2023.

Coley, C. W. Defining and exploring chemical spaces. *Trends in Chemistry*, 3(2):133–145, 2021. ISSN 2589-5974. doi: <https://doi.org/10.1016/j.trechm.2020.11.004>. URL <https://www.sciencedirect.com/science/article/pii/S2589597420302884>. Special Issue: Machine Learning for Molecules and Materials.

Degen, J., Wegscheid-Gerlach, C., Zaliani, A., and Rarey, M. On the art of compiling and using “drug-like” chemical fragment spaces. *ChemMedChem*, 3(10): 1503–1507, October 2008. ISSN 1860-7187. doi: 10.1002/cmdc.200800178. URL <http://dx.doi.org/10.1002/cmdc.200800178>.

Ertl, P. and Schuffenhauer, A. Estimation of synthetic accessibility score of drug-like molecules based on molecular complexity and fragment contributions. *Journal of Cheminformatics*, 1(1), June 2009. ISSN 1758-2946. doi: 10.1186/1758-2946-1-8. URL <http://dx.doi.org/10.1186/1758-2946-1-8>.

Fey, M. and Lenssen, J. E. Fast graph representation learning with PyTorch Geometric. In *ICLR Workshop on Representation Learning on Graphs and Manifolds*, 2019.

Francoeur, P. G., Masuda, T., Sunseri, J., Jia, A., Iovanisci, R. B., Snyder, I., and Koes, D. R. Three-dimensional convolutional neural networks and a cross-docked data set for structure-based drug design. *Journal of Chemical Information and Modeling*, 60(9):4200–4215, August 2020. ISSN 1549-960X. doi: 10.1021/acs.jcim.0c00411. URL <http://dx.doi.org/10.1021/acs.jcim.0c00411>.

Gentile, F., Agrawal, V., Hsing, M., Ton, A.-T., Ban, F., Norinder, U., Gleave, M. E., and Cherkasov, A. Deep docking: a deep learning platform for augmentation of structure based drug discovery. *ACS central science*, 6 (6):939–949, 2020.

Girshick, R. Fast r-cnn. In *Proceedings of the IEEE international conference on computer vision*, pp. 1440–1448, 2015.

Goel, M., Raghunathan, S., Laghuvarapu, S., and Priyakumar, U. D. MoleGuLAR: Molecule generation using reinforcement learning with alternating rewards. *Journal of Chemical Information and Modeling*, 61(12): 5815–5826, December 2021. doi: 10.1021/acs.jcim.1c01341. URL <https://doi.org/10.1021/acs.jcim.1c01341>.

Guan, J., Qian, W. W., Peng, X., Su, Y., Peng, J., and Ma, J. 3d equivariant diffusion for target-aware molecule generation and affinity prediction. In *ICLR*, 2023a.

Guan, J., Zhou, X., Yang, Y., Bao, Y., Peng, J., Ma, J., Liu, Q., Wang, L., and Gu, Q. Decompdiff: Diffusion models with decomposed priors for structure-based drug design. *ICML*, 2023b.

Harris, C., Didi, K., Jamasb, A. R., Joshi, C. K., Mathis, S. V., Lio, P., and Blundell, T. Benchmarking generated poses: How rational is structure-based drug design with generative models?, 2023.

Hu, W., Liu, B., Gomes, J., Zitnik, M., Liang, P., Pande, V., and Leskovec, J. Strategies for pre-training graph neural networks. *arXiv preprint arXiv:1905.12265*, 2019.

Huey, R., Morris, G. M., and Forli, S. Using autodock 4 and autodock vina with autodocktools: a tutorial. *The Scripps Research Institute Molecular Graphics Laboratory*, 10550(92037):1000, 2012.

Irwin, J. J., Tang, K. G., Young, J., Dandarchuluun, C., Wong, B. R., Khurelbaatar, M., Moroz, Y. S., Mayfield, J., and Sayle, R. A. Zinc20—a free ultralarge-scale chemical database for ligand discovery. *Journal of chemical information and modeling*, 60(12):6065–6073, 2020.

Jain, M., Raparthy, S. C., Hernandez-Garcia, A., Rector-Brooks, J., Bengio, Y., Miret, S., and Bengio, E. Multi-objective gflownets, 2023.

Jeon, W. and Kim, D. Autonomous molecule generation using reinforcement learning and docking to develop potential novel inhibitors. *Scientific Reports*, 10(1), December 2020. doi: 10.1038/s41598-020-78537-2. URL <https://doi.org/10.1038/s41598-020-78537-2>.

Jin, W., Barzilay, R., and Jaakkola, T. S. Junction tree variational autoencoder for molecular graph generation. *CoRR*, abs/1802.04364, 2018. URL <http://arxiv.org/abs/1802.04364>.

Jing, B., Eismann, S., Suriana, P., Townshend, R. J. L., and Dror, R. Learning from protein structure with geometric vector perceptrons, 2021.

Jumper, J., Evans, R., Pritzel, A., Green, T., Figurnov, M., Ronneberger, O., Tunyasuvunakool, K., Bates, R., Žídek, A., Potapenko, A., et al. Highly accurate protein structure prediction with alphafold. *Nature*, 596(7873):583–589, 2021.

Kingma, D. P. and Ba, J. Adam: A method for stochastic optimization, 2017.

Landrum, G. et al. Rdkit: Open-source cheminformatics, 2006.

Lau, E., Vemgal, N. M., Precup, D., and Bengio, E. DGFN: Double generative flow networks. In *NeurIPS 2023 Generative AI and Biology (GenBio) Workshop*, 2023. URL <https://openreview.net/forum?id=1wa9JEanV5>.

Lee, S., Jo, J., and Hwang, S. J. Exploring chemical space with score-based out-of-distribution generation. In *International Conference on Machine Learning*, pp. 18872–18892. PMLR, 2023.

Li, S., Wan, F., Shu, H., Jiang, T., Zhao, D., and Zeng, J. Monn: a multi-objective neural network for predicting compound-protein interactions and affinities. *Cell Systems*, 10(4):308–322, 2020.

Lipinski, C. A., Lombardo, F., Dominy, B. W., and Feeney, P. J. Experimental and computational approaches to estimate solubility and permeability in drug discovery and development settings. *Advanced Drug Delivery Reviews*, 23(1):3–25, 1997. ISSN 0169-409X. doi: [https://doi.org/10.1016/S0169-409X\(96\)00423-1](https://doi.org/10.1016/S0169-409X(96)00423-1). URL <https://www.sciencedirect.com/science/article/pii/S0169409X96004231>. In Vitro Models for Selection of Development Candidates.

Liu, M., Luo, Y., Uchino, K., Maruhashi, K., and Ji, S. Generating 3d molecules for target protein binding. In *ICML*, 2022.

Liu, Z., Li, Y., Han, L., Li, J., Liu, J., Zhao, Z., Nie, W., Liu, Y., and Wang, R. Pdb-wide collection of binding data: current status of the pdbbind database. *Bioinformatics*, 31(3):405–412, October 2014. ISSN 1367-4803. doi: 10.1093/bioinformatics/btu626. URL <http://dx.doi.org/10.1093/bioinformatics/btu626>.

Loshchilov, I. and Hutter, F. Decoupled weight decay regularization. In *International Conference on Learning Representations*, 2018.

Luo, S., Guan, J., Ma, J., and Peng, J. A 3D generative model for structure-based drug design. In *NeurIPS*, 2021.

Malkin, N., Jain, M., Bengio, E., Sun, C., and Bengio, Y. Trajectory balance: Improved credit assignment in gflownets, 2023.

Masuda, T., Ragoza, M., and Koes, D. R. Generating 3d molecular structures conditional on a receptor binding site with deep generative models. *arXiv preprint arXiv:2010.14442*, 2020.

O’Boyle, N. M., Banck, M., James, C. A., Morley, C., Vandermeersch, T., and Hutchison, G. R. Open babel: An open chemical toolbox. *Journal of cheminformatics*, 3(1):1–14, 2011.

Olivecrona, M., Blaschke, T., Engkvist, O., and Chen, H. Molecular de-novo design through deep reinforcement learning. *Journal of Cheminformatics*, 9(1), September 2017. doi: 10.1186/s13321-017-0235-x. URL <https://doi.org/10.1186/s13321-017-0235-x>.

Pandey, M., Radaeva, M., Mslati, H., Garland, O., Fernandez, M., Ester, M., and Cherkasov, A. Ligand binding prediction using protein structure graphs and residual graph attention networks. *Molecules*, 27(16), 2022. ISSN 1420-3049. doi: 10.3390/molecules27165114. URL <https://www.mdpi.com/1420-3049/27/16/5114>.

Paszke, A., Gross, S., Massa, F., Lerer, A., Bradbury, J., Chanan, G., Killeen, T., Lin, Z., Gimelshein, N., Antiga, L., Desmaison, A., Kopf, A., Yang, E., DeVito, Z., Raison, M., Tejani, A., Chilamkurthy, S., Steiner, B., Fang, L., Bai, J., and Chintala, S. Pytorch: An imperative style, high-performance deep learning library. In *Advances in Neural Information Processing Systems 32*, pp. 8024–8035. Curran Associates, Inc., 2019.

Peng, X., Luo, S., Guan, J., Xie, Q., Peng, J., and Ma, J. Pocket2mol: Efficient molecular sampling based on 3d protein pockets. In *ICML*, pp. 17644–17655. PMLR, 2022.

Pham, T., Tran, T., Dam, H., and Venkatesh, S. Graph classification via deep learning with virtual nodes, 2017.

Powers, A. S., Yu, H. H., Suriana, P., Koodli, R. V., Lu, T., Paggi, J. M., and Dror, R. O. Geometric deep learning for structure-based ligand design. *ACS Central Science*, November 2023. ISSN 2374-7951. doi: 10.1021/acscentsci.3c00572. URL <http://dx.doi.org/10.1021/acscentsci.3c00572>.

Pushpakom, S., Iorio, F., Eyers, P. A., Escott, K. J., Hopper, S., Wells, A., Doig, A., Guilliams, T., Latimer, J., McNamee, C., Norris, A., Sanseau, P., Cavalla, D., and Pirmohamed, M. Drug repurposing: progress, challenges and recommendations. *Nature Reviews Drug Discovery*, 18(1):41–58, oct 2018. doi: 10.1038/nrd.2018.168. URL <https://doi.org/10.1038/nrd.2018.168>.

Replogle, J. M., Saunders, R. A., Pogson, A. N., Hussmann, J. A., Lenail, A., Guna, A., Mascibroda, L., Wagner, E. J., Adelman, K., Lithwick-Yanai, G., Iremadze, N., Oberstrass, F., Lipson, D., Bonnar, J. L., Jost, M., Norman, T. M., and Weissman, J. S. Mapping information-rich genotype-phenotype landscapes with genome-scale perturb-seq. *Cell*, 185(14):2559–2575.e28, July 2022. ISSN 0092-8674. doi: 10.1016/j.cell.2022.05.013. URL <http://dx.doi.org/10.1016/j.cell.2022.05.013>.

Schneuing, A., Du, Y., Harris, C., Jamasb, A., Igashov, I., Du, W., Blundell, T., Lió, P., Gomes, C., Welling, M., Bronstein, M., and Correia, B. Structure-based drug design with equivariant diffusion models, 2023.

Schreyer, A. M. and Blundell, T. Usrcat: real-time ultra-fast shape recognition with pharmacophoric constraints. *Journal of Cheminformatics*, 4(1), November 2012. ISSN 1758-2946. doi: 10.1186/1758-2946-4-27. URL <http://dx.doi.org/10.1186/1758-2946-4-27>.

Seo, S. and Kim, W. Y. Pharmaconet: Accelerating large-scale virtual screening by deep pharmacophore modeling, 2023.

Seo, S., Lim, J., and Kim, W. Y. Molecular generative model via retrosynthetically prepared chemical building block assembly. *Advanced Science*, 10(8):2206674, 2023.

Steinegger, M. and Söding, J. Mmseqs2 enables sensitive protein sequence searching for the analysis of massive data sets. *Nature Biotechnology*, 35(11):1026–1028, October 2017. ISSN 1546-1696. doi: 10.1038/nbt.3988. URL <http://dx.doi.org/10.1038/nbt.3988>.

Trott, O. and Olson, A. J. AutoDock Vina: improving the speed and accuracy of docking with a new scoring function, efficient optimization, and multithreading. *Journal of computational chemistry*, 31(2):455–461, 2010.

Wallach, I. and Heifets, A. Most ligand-based classification benchmarks reward memorization rather than generalization. *Journal of chemical information and modeling*, 58(5):916–932, 2018.

Wermuth, C.-G., Ganellin, C., Lindberg, P., and Mitscher, L. Glossary of terms used in medicinal chemistry (iupac recommendations 1998). *Pure and applied Chemistry*, 70(5):1129–1143, 1998.

Yang, S.-Y. Pharmacophore modeling and applications in drug discovery: challenges and recent advances. *Drug discovery today*, 15(11-12):444–450, 2010.

Yun, S., Jeong, M., Kim, R., Kang, J., and Kim, H. J. Graph transformer networks, 2020.

Zhang, H., Saravanan, K. M., and Zhang, J. Z. Deepbindgcn: Integrating molecular vector representation with graph convolutional neural networks for protein–ligand interaction prediction. *Molecules*, 28(12):4691, 2023a.

Zhang, Z. and Liu, Q. Learning subpocket prototypes for generalizable structure-based drug design. In *ICML*, 2023.

Zhang, Z., Min, Y., Zheng, S., and Liu, Q. Molecule generation for target protein binding with structural motifs. In *The Eleventh ICLR*, 2023b.

Zhang, Z., Yan, J., Liu, Q., Chen, E., and Zitnik, M. A systematic survey in geometric deep learning for structure-based drug design, 2023c.

Zhou, Z., Kearnes, S., Li, L., Zare, R. N., and Riley, P. Optimization of molecules via deep reinforcement learning. *Scientific Reports*, 9(1), jul 2019. doi: 10.1038/s41598-019-47148-x. URL <https://doi.org/10.1038%2Fs41598-019-47148-x>.

## A. Softwares

In this study, we used the open-sourced code for GFlowNet (Bengio et al., 2021), PharmacoNet (Seo & Kim, 2023) and GVP-GNN (Jing et al., 2021). Our models were implemented using the Pytorch (Paszke et al., 2019) and PyTorch Geometric (Fey & Lenssen, 2019) libraries, which enabled efficient training and evaluation. We utilized RDKit (Landrum et al., 2006), a widely-used chem-informatics library, to handle the molecular structures and compute chemical properties. We employed the QuickVina 2.1 (QVina) (Alhossary et al., 2015) for docking, and used Openbabel (O’Boyle et al., 2011) and AutoDock Tools (Huey et al., 2012) to generate ready-to-dock files.

## B. Additional details of pocket conditioned GFlowNet

### B.1. Action sampling

We present the action sampling process below:

$$\mathbf{a}_{Add} = MLP \left( \mathbf{h}^{L(N)} \right) \quad (6)$$

$$\mathbf{a}_{Attach} = MLP \left( \mathbf{e}^{L(N)} \right) \quad (7)$$

$$\mathbf{a}_{Stop} = MLP \left( \mathbf{g}^{L(N)} \right) \quad (8)$$

$$\pi(\mathbf{a} | \mathcal{G}_t^L, \mathbf{h}_{\mathcal{G}^P}) = softmax(Concat(\mathbf{a}_{Add}, \mathbf{a}_{Attach}, \mathbf{a}_{Stop})) \quad (9)$$

$$a \sim \pi(\mathbf{a} | \mathcal{G}_t^L, \mathbf{h}_{\mathcal{G}^P}) \quad (10)$$

### B.2. Reward function

We normalize SA score using the formula  $\frac{10-SA}{9}$  to obtain  $\widehat{SA}$ . We also multiply the predicted docking score by  $-1$  to obtain a positive affinity reward  $\widehat{DS}$ . While  $QED$  and  $SA$  need to meet a certain threshold to make a good drug molecule, optimizing these values beyond the threshold does not bring additional utility (Coley, 2021). Therefore, we give no additional rewards to a molecule for having a  $QED$  or  $SA$  beyond  $QED_{sat}$  and  $SA_{sat}$  respectively. As the docking scores that indicate high affinity differ across pockets, we first compute  $\overline{DS}$ , which is the mean docking score of 1,000 random ZINC molecules for the given pocket, also multiplied by  $-1$ . Next, we normalize the docking score improvement of a given molecule and pocket by subtracting  $\overline{DS}$  from  $\widehat{DS}$ . We clip this docking score improvement compared to a random molecule to be  $\geq 0$ . To avoid a constant 0 affinity improvement reward for all molecules that perform below average, we introduce a hyperparameter  $\gamma$ , which scales the docking score reward gained from docking score without mean subtracted. We use the following settings for all experiments:  $QED_{sat} = 0.7$ ,  $SA_{sat} = 0.8$ , and  $\gamma = 0.2$ . Formally the reward is defined as follows:

$$QED_{reward} = \begin{cases} 1, & \text{if } QED > QED_{sat} \\ \frac{QED}{QED_{sat}}, & \text{else} \end{cases}$$

$$SA_{reward} = \begin{cases} 1, & \text{if } SA > SA_{sat} \\ \frac{SA}{SA_{sat}}, & \text{else} \end{cases}$$

$$DS_{reward} = \begin{cases} \widehat{DS} - \overline{DS} + \gamma \widehat{DS}, & \text{if } \widehat{DS} < \overline{DS} \\ \gamma \widehat{DS}, & \text{else} \end{cases}$$

$$Reward = QED_{reward} \times SA_{reward} \times DS_{reward}$$

### B.3. Model Details

We use Double GFN (Lau et al., 2023) to improve exploration in sparse reward domains and high-dimensional states. Our model is trained via the gradient descent method Adam (Kingma & Ba, 2017). We list hyperparameters used in Table 5 and compare the training time of our method in Table 6.

Table 5. Hyperparameters used for target conditional GFlowNet

Hyperparameters	Values
Num of training steps	30,000
Learning rate	$10^{-4}$
Weight decay	$10^{-8}$
Momentum	0.9
Adam eps	$10^{-8}$
Sampling $\tau$	0.99
Learning rate $Z$ -estimator	$10^{-3}$
Max nodes	9
Random action prob	0.01
Batch size	8
Temp sampling distribution	<i>Uniform</i> (0, 64)
Pocket cond dim	128
Transformer hidden dim	256
Num of transformer layers	2

Table 6. Comparison of training time.

Model	Total Steps	Batch Size	Total Time (hrs)	Hardware
Pocket2Mol	475k	8	72.6	GTX A100 80GB
TargetDiff	300k	4	25.0	GTX A100 80GB
DecompDiff	300k	4	41.7	GTX A100 80GB
TACOGFN	30k	8	17.7	RTX 3090 24GB

## C. Additional details of docking score predictor

### C.1. Motivation

When developing a docking score prediction model, two essential requirements are its speed of processing and its applicability to a variety of proteins and ligands. Since the binding poses are computationally or experimentally expensive, previous affinity prediction models or docking score prediction models (Zhang et al., 2023a) predict energy by integrating the 1D representation vectors  $\mathbf{z}^P$  of the protein  $\mathcal{P}$  and  $\mathbf{z}^L$  of ligand  $\mathcal{L}$ , respectively:

$$\mathbf{z}_p = \phi_P(\mathcal{P}) \quad (11)$$

$$\mathbf{z}_l = \phi_L(\mathcal{L}) \quad (12)$$

$$E = \phi_z(\text{Concat}(\mathbf{z}_p, \mathbf{z}_l)) \quad (13)$$

However, this approach can not consider the atom pairwise interactions between ligands and proteins due to global pooling, so it shows less generalizability to unseen ligands or proteins. Compared to previous methods, MONN (Li et al., 2020) proposed a pairwise interaction map  $\mathbf{I}$  between protein amino acid embeddings  $\{\mathbf{h}_i^P\}$  and ligand node embeddings  $\{\mathbf{h}_j^L\}$ :

$$\mathbf{I} = \{\mathbf{h}_i^P\} \odot \{\mathbf{h}_j^L\} \quad (14)$$

$$E = \text{SumPool}(\phi_{\mathbf{I}}(\mathbf{I})) \quad (15)$$

However, the use of full amino acid sequences is computationally expensive for large proteins. Furthermore, in target-based drug design tasks that prioritize binding pocket information, affinity prediction over the entire protein can sometimes lead to incorrect energy calculations for different pockets. Therefore, our study adopts the use of pharmacophores within the binding pocket as an alternative to considering the entire protein sequence. This approach not only effectively captures the unique features of the protein pocket, but also simplifies its topology, thereby addressing the computational burden and the generalization issues. Also, conceptually our docking score predictor determines whether a ligand atom corresponds to each pharmacophore node rather than whether it forms non-covalent interactions with each amino acid or atom.

### C.2. Training details

For model training, we use 15% of pocket in the training set for the validation set. We used AdamW (Loshchilov & Hutter, 2018) optimizer with betas of (0.9, 0.999) and a weight decay of 0.05, and a learning rate is 0.0001 with a decaying factor of 0.1 per 20,000 iterations. Each iteration has 32 randomly sampled pockets and 128 randomly selected ligands for each pocket during training on ZINCDock-15M. For CrossDock-100k, we used up to 4 ligands per pocket. We optimize our model with SmoothL1Loss (Girshick, 2015) for 100,000 iterations and select the best model weights with the lowest validation loss. The training process takes about a day on 4 NVIDIA RTX A4000 GPUs.

### C.3. Performance of docking score prediction model

To evaluate the performance of our docking score predictor, we use two test sets: **CrossDocked-100k-test** and **ZINCDock-test**. **CrossDocked-100k-test** is the test set of CrossDocked-100k dataset used in (Luo et al., 2021) and contains one ligand per each pocket. We re-docked each test ligand to perform the evaluation in the same environment as the generation process. **ZINCDock-test** is the docking simulation data of randomly selected 100 ZINC20 molecules for each pocket in CrossDocked-100k-test. The size of the test sets is 100 pocket-ligand pairs for the CrossDocked-100k-test and 10,000 pocket-ligand pairs for the ZINCDock-test.

Table 7. The evaluation of docking score prediction performance of predictor trained on two different docking score datasets.

Test set	Training set	RMSE (kcal/mol)	MAE (kcal/mol)	Pearson	Spearman
CrossDocked-100k-test	CrossDocked-100k	0.881	0.652	0.918	0.913
	ZINCDock-15M	1.143	0.880	0.867	0.828
ZINCDock-test	CrossDocked-100k	1.121	0.791	0.749	0.790
	ZINCDock-15M	0.862	0.574	0.805	0.846

## D. Additional experiment details

### D.1. Dataset

CrossDocked (Francoeur et al., 2020) is a dataset containing 22.5 million poses of ligands docked into multiple similar binding pockets from PDBBind. For **CrossDocked-100k** set, we use an identical processing strategy to previous works (Luo et al., 2021; Peng et al., 2022): First, data points with binding pose RMSD greater than 1Å are filtered. Then, mmseq2 (Steinegger & Söding, 2017) is to cluster data at 30% sequence identity. After splitting, 100,000 protein-ligand pairs are randomly drawn for the training set. 100 test pockets are drawn from the remaining pocket clusters. 15,307 unique protein pockets remain in the training set.

### D.2. Docking protocol

In some previous evaluation protocols, the generated 3D molecules from the model are directly used as the conformations for the re-docking process. However, these generated 3D conformations may contain unrealistic bond length or bond angles (Harris et al., 2023) and therefore produce distorted docking scores. It is more reasonable and realistic to first calculate a conformer with realistic geometry, which is a necessary step in standard docking protocols, before docking (Bender et al., 2021). For our protocol, we first convert all generated molecules into SMILES and calculate their ETKDG conformers (srETKDGv3) using RDKit. Then, we prepare ready-to-dock files of ligands and proteins with Openbabel and AutoDockTools (O’Boyle et al., 2011; Huey et al., 2012). Finally, we dock these conformers using Quick VINA 2.1 (QVina) (Trott & Olson, 2010; Alhossary et al., 2015). For QVina, we use a box size of 20 Å and an exhaustiveness of 8.

### D.3. Experimental metric details

Some baseline methods did not generate at least 10 molecules which satisfy the *desirable* criteria for a number of pockets. To compute **Top-10 Desr. DS** in these cases, a docking score of 0 is used as a placeholder for the top 10 docking scores.

### D.4. Baseline evaluations

For our baseline generation, we selected Pocket2Mol (Peng et al., 2022), TargetDiff (Guan et al., 2023a), DecompDiff (Guan et al., 2023b). We adhered to the default hyperparameter settings for all models. DecompDiff incorporates three prior modes: subpocket, reference, and beta. Of these, we selected the beta mode for our analysis, as it demonstrated the highest docking score, aligning with findings reported in its original publication.

We generated 100 molecules for each of the 100 protein pockets from the Crossdock2020 (Francoeur et al., 2020) test set. Following generation, we applied a filtering process to ensure that all molecules were unique and met validity criteria. Molecules were deemed invalid and discarded, if they had reconstruction errors, were duplicates, or were disconnected. The remaining SMILES obtained from these models were compiled to establish the baseline. We then proceeded to perform the docking protocol on each of the SMILES to obtain their respective docking scores. Our results were in line with those reported in the original studies of the respective models.

## D.5. Additional Results

### D.5.1. GENERATED SAMPLES

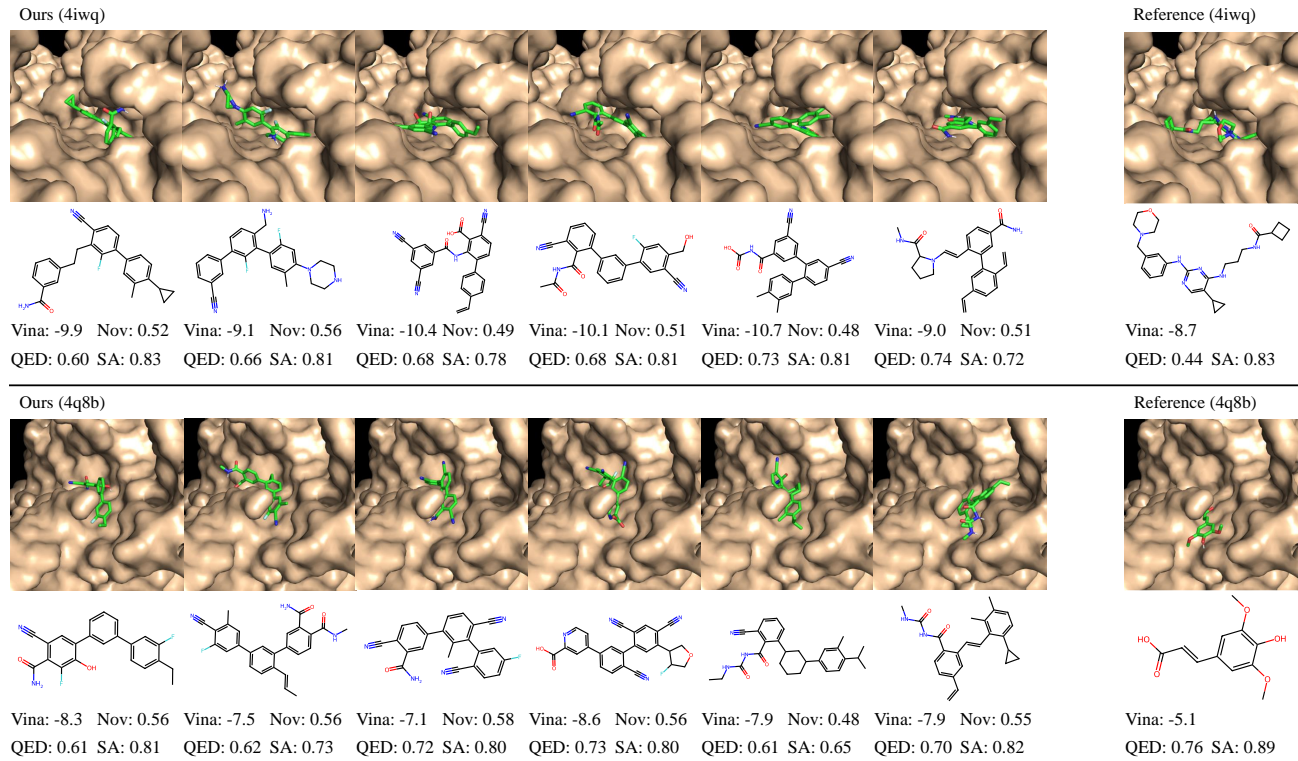


Figure 5. To present of fair a overview of the model performance, we selected *4iwq* and *4q8b* at the 25-th and 75-th percentiles based on their docking scores with native ligands. We show compare the molecules generated by TACOGFN against the native ligand with their QED, SA, Novelty, and Docking score (Vina).

### D.5.2. GENERATION QUALITY

To measure the quality of molecule generation, we generated 100 molecules for each test pocket with state-of-the-art methods. Note that we do not resample the molecules until the number of valid and novel molecules reaches 100, in contrast to Section 5.2. Validity is defined as being readable by RDKit and successful in docking. We measured the average percentages of unique and valid molecules in the generated samples.

Table 8. The valid & unique is the average percentage of valid and unique molecules out of the 100 generated samples.

Model	valid & unique (%)
Pocket2Mol (Peng et al., 2022)	71.86
TargetDiff (Guan et al., 2023a)	91.45
DecompDiff (Guan et al., 2023b)	66.32
TACOGFN	100.00